Article:
Carcadea, E., Varlam, M., Marinoiu, A. et al. (2019) Influence of catalyst structure on PEM fuel cell performance – A numerical investigation. International Journal of Hydrogen Energy, 44 (25). pp. 12829-12841. ISSN: 0360-3199

https://doi.org/10.1016/j.ijhydene.2018.12.155

Influence of catalyst structure on PEM fuel cell performance – a numerical investigation

E. Carcadea[a*], M. Varlam[a], A. Marinoiu[a], M. Raceanu[a], M. S. Ismail[b] and D.B. Ingham[b]
[a]National Research and Development Institute for Cryogenics and Isotopic Technologies - ICSI Rm. Valcea, 240050, Romania
[b]Energy2050, Department of Mechanical Engineering, Faculty of Engineering, University of Sheffield, Sheffield S10 2TN, UK
(*) elena.carcadea@icsi.ro

Abstract

The effect of the catalyst microstructure on a 5 cm^2 PEM fuel cell performance is numerically investigated. The catalyst layer composition and properties (i.e. ionomer volume fraction, platinum loading, particle radius, electrochemical active area and carbon support type), and the mass transport resistance due to the ionomer and liquid water surrounding the catalyst particles, are incorporated into the model. The effects of the above parameters are discussed in terms of the polarization curves and the local distributions of the key parameters. An optimum range of the ionomer volume fraction was found and a gain of 39% in the performance was achieved. As regards the platinum loading and catalyst particle radius, the results showed that a higher loading and a smaller radius leads to an increase in the PEMFC performance. Further, the influence of the electrochemical active area produces an overall increase of 22% in current density and this was due to the use of a new material developed as support for Pt particles, an iodine doped graphene, which has better electrical contacts and additional pathways for water removal. Using this parameter, the numerical model has been validated and good agreement with experimental data was achieved, thus giving confidence in the model as a design tool for future improvements of the catalyst structure.

Keywords: PEM fuel cell; numerical model; catalyst microstructure; ionomer volume fraction; platinum loading; electrochemical active area.

1. Introduction

Proton Exchange Membrane (PEM) Fuel Cells are promising power conversion technologies for automotive and stationary backup applications and this is mainly due to their high power density and low temperature operation (<100 °C). An essential part in the PEM fuel cells development and commercialization is the use of an appropriate catalyst that meets certain requirements: high performance, low cost and high durability. The noble metals (platinum) are commonly used as catalysts due to their high chemical stability and high exchange current density, but because they are expensive and can be easily poisoned then alternatives would be advantageous. Developing new electrodes with reduced load or no platinum is still a topic of great scientific interest and, therefore, further numerical and experimental studies are still necessary to fulfil this goal [1-3].

PEM Fuel Cells are electrochemical devices that convert the chemical energy of a fuel and oxidant directly to electric energy, with heat and water as by-products. The electrochemical reactions take place in the catalyst layers (CL). At the anode catalyst the hydrogen molecules separate into protons and electrons. The protons flow through the electrolyte to reach the cathode side and the electrons flow through an external circuit and generate electric power. At the cathode catalyst the supplied oxygen combines with the protons and electrons and generate water and heat. For promoting these reactions, the catalyst layers must have a high active surface area and an adequate microstructure to allow for the transport of reactants, ions, electrons and by-products. The catalyst layer microstructure can be described as a group of agglomerates that consists of four different elements: carbon particles, Pt particles, an ionomer network and pores, see Fig. 1. Each of these phases play an important role in the key processes occurring within the entire fuel cell, starting from the diffusion of gases through pores and in the ionomer film; from the water absorption by the ionomer or water diffusion back to the pore; from proton and electron transfer through the ionomer film and carbon/platinum, respectively; up to the heat transfer from the reaction site towards the gas channel [4]. Some critical factors, such as: mass transport resistance caused by the ionomer and liquid water

films surrounding the catalyst particles, Pt loading, Pt and carbon particle sizes, ionomer volume fraction and CL porosity, must be considered when the PEM fuel cell performance and durability are being evaluated [5-8].

The catalyst layer is a group of agglomerates that creates a porous network. The size of each agglomerate is about 200 nm [9-10]. There is void space inside each agglomerate, called primary pores (< 20 nm), and void space between agglomerates, called secondary pores (>20 nm). The primary pores include micropores (<2 nm) that can be blocked by Pt particles [11-12] and mesopores (2-20 nm) that are partially occupied by the ionomer [13]. The secondary pores are relatively large and are available for gas transport.

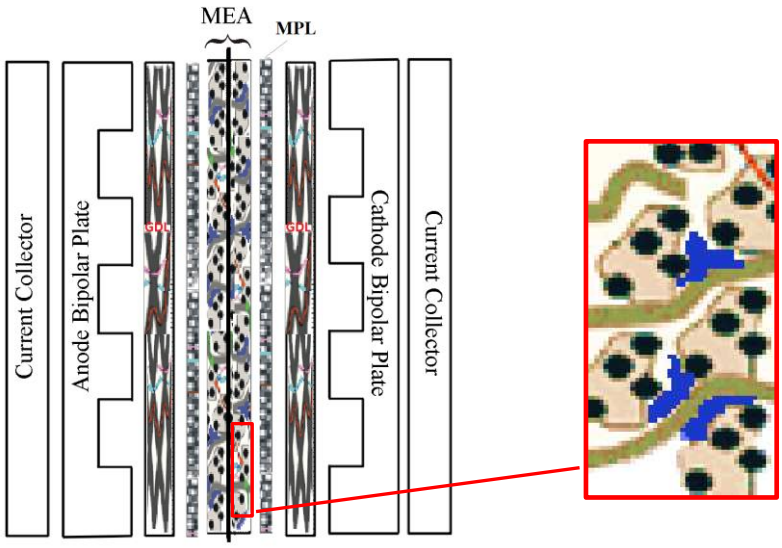

Fig. 1 – Schematic of the PEM fuel cell components with a zoom of the catalyst layer microstructure.

One way to investigate the influence of the catalyst microstructure on the PEM fuel cell performance is through performing numerical simulations. There are three different categories of models that can be used to account for the catalyst layer: thin-film [14-15], macro-homogeneous [16-17] and agglomerate models [18-21]. A comparison of these models [22] shows that the catalyst agglomerate model is the only model that is capable of capturing all the mass transport losses; the thin film and the macro-homogeneous models overpredict the fuel cell performance. This is because the use of a thin film for the catalyst layer prevents considering any kind of transport or resistance in the physical structure of the catalyst layer. On the other hand, the macro-homogeneous model does not consider the formation of agglomerates. Therefore no reactant dissolution at the gas/ionomer interface, nor diffusion and reaction within the agglomerate structure are taken into account. The agglomerate model includes all possible transport phenomena that takes place into the CL such us: gas-phase transport in the pore space of the catalyst layer; dissolution of reactants in the electrolyte phase; simultaneous diffusion and reaction of the dissolved reactant within the agglomerate; ion transport in the electrolyte phase; and electron conduction via the carbon black particles.

A key factor that determines both the electrocatalytic activity and the durability of carbon supported Pt electrocatalysts used in PEM fuel cells is related to the Pt loading and Pt particle size. The goal of the research carried out in developing catalysts for PEM fuel cells is to reduce the platinum loading to 0.125 mg/cm^2 or even to lower values by 2020 [23]. High platinum loadings lead to a fast reaction rate for the oxygen reduction reaction due to the additional catalytic surface area provided. If Pt loading is to be reduced, it is necessary to keep the high catalyst active surface area and one way to achieve this is to reduce the platinum particle size [24-25]. Analyzing the effect of the Pt particle size on the activity for ORR have been reported in several papers [5, 20, 27-29]. An optimum Pt particle size of 4 nm for the maximum ORR mass activity was found by Peuckert et al.

[26] and a significant decrease in performance when reducing the particle size to 1 nm. These results are in good agreement with the findings of Malek et al. [12] who suggest a range between 2-5 nm for maximum ORR mass activity; such particle size was used as a fitting parameter for the respective mathematical models. Soboleva et al. [11] found that the distribution of Pt particles is dependent on the porous structure of the carbon support. In another work [50] no Pt particle size effect was noticed even if the radius decreased to 1.4 nm. These contradictory results leads to the conclusion that a comprehensive investigation for evaluating the effect of catalyst layer microstructure on the PEM fuel cell performance is still required.

Another important parameter in evaluating the PEM fuel cell performance is the ionomer volume fraction of the CL. The ionomer network acts as a pathway for protons in reaching the reaction sites and as a diffusive medium for the oxygen gas. Different values for the ionomer content have been investigated and an optimum ionomer volume fraction of the electrodes that offer an increased PEM fuel cell performance was found [29-31]. The ionomer is a binder for the Pt and carbon particles; therefore, each of these components must be analyzed. Carbon based materials are used as catalyst support for the dispersed Pt particles and for conducting the electrons to the reaction sites, the carbon black being the most commonly used. A mesoporous carbon substrate with the pore diameters in the range 2-20 nm is considered adequate for placing the Pt particles because it allows a better mass transfer and have optimum properties (good electrical and thermal conductivity, and high porosity) [32]. If the carbon support has micropores (<2 nm), the Pt particles can block the entrance of these micropores, thus cancelling the effect of the pores. In this case the micropores are considered active sites for platinum deposition without contributing to the improvement of the fuel cell performance [11]. An improved support based on nanostructured carbon can be used to replace the usual carbon black supports and graphene is a promising material that can be used due to its unique two-dimensional structure and extraordinary properties (high electronic and thermal conductivity, high surface area and high mechanical strength). The research carried out in the last few years by our group [33,51-53] and others [34-36] on the use of graphene based materials as catalyst layers for PEM fuel cells have demonstrated that a better performance can be achieved due to an increased electrochemical active area and this is due to more platinum sites being available for oxygen reduction reaction. The performance improvement is also due to the graphene structure which benefits from a large number of vacancies and mesopores that offer new channels for reactant and product transport, and ensures conductive paths for the ions and electrons.

Since all these parameters can influence each other, a sensitivity analysis to investigate the effect of the catalyst layer microstructure on the PEM fuel cell performance is required. A CFD model was developed and numerical simulations were carried out in order to investigate the effects of Pt loading, Pt particle radius, ionomer volume fraction, and carbon support on the PEM fuel cell performance. The results are presented in terms of polarization curve plots and profile distributions of the key variables (current density, species, water content and liquid water) and discussed. By optimizing the catalyst layer composition, the performance of the catalyst layer can be improved and also its durability may be increased.

2. Mathematical Model Development

The fuel cell model is based on the conservation of mass, momentum, species, charge and energy [37]. These transport equations are coupled with electrochemical processes through source terms. The mathematical modelling is based on a previously developed model [38], assuming: 3-dimensional investigation, operation under steady state conditions, incompressible and laminar flow for the fuel and air. A comprehensive two-phase model for PEM fuel cells must account for the modelling transport of all three water phases (gaseous, liquid and dissolved). Also, the mass transport resistance due to the catalyst microstructure, the liquid water transport through hydrophobic porous layers and the two-phase flow (liquid saturation) in the gas channels must be considered and are taken into account in the proposed model, being incorporated in the cathode particle model presented in Section 2.1.

Additional assumptions are employed in this study in order to take into account the microstructure of the catalyst layers [10, 28, 39]:

- the catalyst layer is assumed to be formed of spherical agglomerates that consist in platinum dispersed carbon, ionomer and void.
- the primary pores, which exist inside each agglomerate, are completely filled with ionomer, allowing for dissolved oxygen diffusion and proton transfer.
- the secondary pores, formed between the agglomerates within the CL, are partially occupied by the ionomer and liquid water.

The following parameters have been considered in developing the model:

- Liquid water saturation, s, is the volume fraction of the secondary pores filled with liquid water
- Platinum loading and carbon loading are denoted by m_{Pt} and m_C, respectively
- The Pt, C and ionomer volume fractions in the CL are denoted by ε_{Pt}, ε_C and $\varepsilon_{N,CL}$
- The GDL penetration into the CL due to the fuel cell assembly is accounted for as a volume fraction, $L_{GDL,CL}$
- The CL thickness is denoted by δ_{CL}.

2.1 The Cathode Particle Model

In the governing equations associated with the mass transport resistance due to the catalyst microstructure, the possible interactions with all water phases are taken into account in the proposed model by replacing the general formulation of the Butler-Volmer function for computing the exchange current density with the Eqs. (1) - (4) [40].

The exchange current density inside the cathode catalyst is one of the most important parameters in defining the electrochemical reaction kinetics because it contains information related to the catalytic activity of the Pt catalyst and to the CL morphology (electrochemical active Pt surface area (ECSA), particle radius), being the link between the macroscopic electrochemical model and the CL microstructure. Therefore, the exchange current density in the cathode catalyst is not based on the general formulation of the Butler-Volmer function [37], but it is calculated using the Eqs. (1) - (4) [40]. It can be noticed that the electrochemical behavior depends on the amount of liquid water produced inside the porous CL structure, on the Pt particle radius and on the ionomer resistance.

$$j_c = 4Fc_{O_2} \Big/ \left(c_{O_2} / j_{O_2}^{ideal} + R_{ion} + R_{liq} \right) \tag{1}$$

$$j_{O_2}^{ideal} = j_c^0 / 4F \tag{2}$$

$$j_c^0 = \left(\zeta_c \cdot j_c^{ref} \right) \left(c_{O_2} / c_{O_2}^{ref} \right) \left[-\exp\left(\alpha_a F \eta_c / RT \right) + \exp\left(-\alpha_c F \eta_c / RT \right) \right] \tag{3}$$

$$R_{liq} = \left(\zeta_c \cdot r_p^2 / \left(K_w \cdot D_w \right) \right) \cdot \left(\left(\sqrt[3]{1 + s\varepsilon_{CL} / \left(1 - \varepsilon_{CL} \right)} - 1 \right) / 3 \cdot \left(1 - \varepsilon_{CL} \right) \right) \tag{4}$$

where R_{ion} is the resistance due to an ionomer film, given from experiments [41], c_{O_2} is the concentration of oxygen, $j_{O_2}^{ideal}$ is the ideal transfer current computed using the Butler-Volmer formulation [37] without any resistance, R_{liq} is the resistance due to the liquid water film surrounding the catalyst particles, $\zeta_c (\frac{m_{Pt}^2}{m_{CL}^3})$ is the specific active surface area for the catalyst, ε_{CL} is the catalyst layer porosity, r_p is the particle radius (m) and $K_w \cdot D_w$ (m^2/s) accounts for the oxygen solubility and diffusivity in the liquid water. The specific active surface area of the catalyst, ζ_c, is related to the electrochemical active surface (a_{ECSA} (m^2/g)) and to the Pt loading (m_{Pt} (g/m^2)) [41] by:

$$\zeta_c = (a_{ECSA} \cdot m_{Pt})/\delta_{CL} \quad (5)$$

The Pt particle radius, r_p (m), is given by the following expression [6]:

$$r_p = 3/(\rho_{Pt} \cdot a_{ECSA}) \quad (6)$$

2.2 Algebraic equations for phase composition

The catalyst layer porosity is determined taking into account its composition: platinum dispersed carbon, ionomer and void [28]:

$$\varepsilon_{CL} = 1 - \varepsilon_{N,CL} - L_{GDL,CL} \cdot (1 - \varepsilon_{GDL}) - \varepsilon_{Pt} - \varepsilon_C \quad (7)$$

$$\varepsilon_{Pt} = m_{Pt}/(\delta_{CL} \cdot \rho_{Pt}) \quad (8)$$

$$\varepsilon_C = m_{Pt} \cdot (1 - f)/(f \cdot \delta_{CL} \cdot \rho_C) \quad (9)$$

$$f = m_{Pt}/(m_{Pt} + m_C) \quad (10)$$

where ρ_{Pt}, ρ_C and ρ_N are the Pt, carbon and ionomer/nafion densities and f is the platinum mass loading to that of platinum and carbon.

The catalyst microstructure parameters detailed in Sections 2.1 and 2.2 are integrated into the PEM fuel cell model developed in our previous study [38] and used to investigate the effect of various structural parameters on the PEM fuel cell performance.

3. Numerical Implementation and boundary conditions

The commercial CFD software ANSYS Fluent 17.0 was used in the numerical investigation [42]. For all the simulations, a set of parameters and operating conditions has been specified as the base case, see Table. Also, all the numerical calculations are performed under the appropriately specified boundary conditions in order to ensure the uniqueness of the governing partial differential equations solution. Dirichlet boundary conditions for the mass flow rate, temperature, relative humidity and mass fractions were prescribed for the channel inlets; see Table 2. On the lateral walls, the solid phase potential was set to be 0 V at the anode side and a value between 0 V and the open circuit voltage at the cathode side.

Since a single computational domain is used, the continuity in the fluxes of all the variables at the interfaces between all the components of the model is ensured. The coupled set of governing equations is iteratively solved until a converged solution is obtained (when the difference between two consecutive residuals is less than 10^{-6} and the difference between the current produced in the anode CL and cathode CL is less than 10^{-4}. The computations were performed using parallel processing of ANSYS Fluent with 32 processes shared on 2 workstations, each with two 8- core processors of 2.6 GHz and 64 GB of RAM. Based on these high- performance computing 2 hours were required for simulating 1 point of the polarization curve.

Table 1. The parameters used in the base case of the model.

Parameter	Value	Unit
Porosity of GDL/MPL/CL	0.7/ /0.6/0.5	-
Permeability of GDL/MPL/CL (K)	$3\times10^{-12}/1\times10^{-12}/2\times10^{-13}$	m^2
Reference exchange current density at anode (j_a^{ref})	3000	A/m^2

Reference exchange current density at cathode (j_c^{ref})	0.3	A/m^2
H_2 molar concentration ($c_{H_2}^{ref}$)	54.6×10^{-3}	kmol/m^3
O_2 molar concentration ($c_{O_2}^{ref}$)	3.39×10^{-3}	kmol/m^3
Anodic transfer coefficient (α_a)	1	-
Cathodic transfer coefficient (α_c)	0.8	-
Contact angle GDL/MPL/CL (θ_c)	110/130/95	^{0}
Anode/cathode specific surface area (ζ_c)	calculated	m_{Pt}^2/m_{CL}^3
Weight fraction of platinum in Pt/C (f)	0.2	-
Platinum mass loading (m_{Pt})	2	g/m2
Ionomer volume fraction in CL ($\varepsilon_{N,CL}$)	15	%
Open circuit voltage (V_{oc})	0.938	V
Membrane thickness	56	µm
GDL thickness	350	µm
MPL thickness	50	µm
Catalyst layer thickness	5.4	µm
Liquid water diffusion coefficient (D_{liq})	1×10^{-5}	m^2/s
Dry membrane density (ρ_i)	2000	kg/m^3
Equivalent weight of the membrane (EW)	1100	kg/kmol

Table 2 The boundary conditions used in the model.

Parameter	Value	Unit
Mass flow rate at anode inlet	8×10^{-7}	kg/s
Mass flow rate at cathode inlet	8×10^{-6}	kg/s
Mass fraction for H_2 at anode inlet	0.475	-
Mass fraction for H_2O at anode inlet	0.525	-
Mass fraction for O_2 at cathode inlet	0.242	-
Mass fraction for H_2O at cathode inlet	0.0699	-
Relative humidity at anode/cathode inlets	56 %	-
Temperature at anode/cathode inlets	60	°C

The computational domain presented in Fig. 2 was developed using the Gambit® 2.4.6 software, the mesh developed having about 1.1 million hexahedral cells and being refined until mesh-independent solutions were obtained. The 5 cm^2 geometry design of the fuel cell numerically investigated is based on the dimensions of a real fuel cell. The same configuration of the flow fields in the anode and cathode sides, namely a 3- pass serpentine, have been used in our numerical and experimental investigations. Each gas channel has 0.5 mm width and 0.5 mm depth. In the area where the parallel channels connects each other a different depth of 1 mm is used. The bipolar plate is 22.5 mm × 22.5 mm in x and y – directions and its thickness is 1.5 mm.

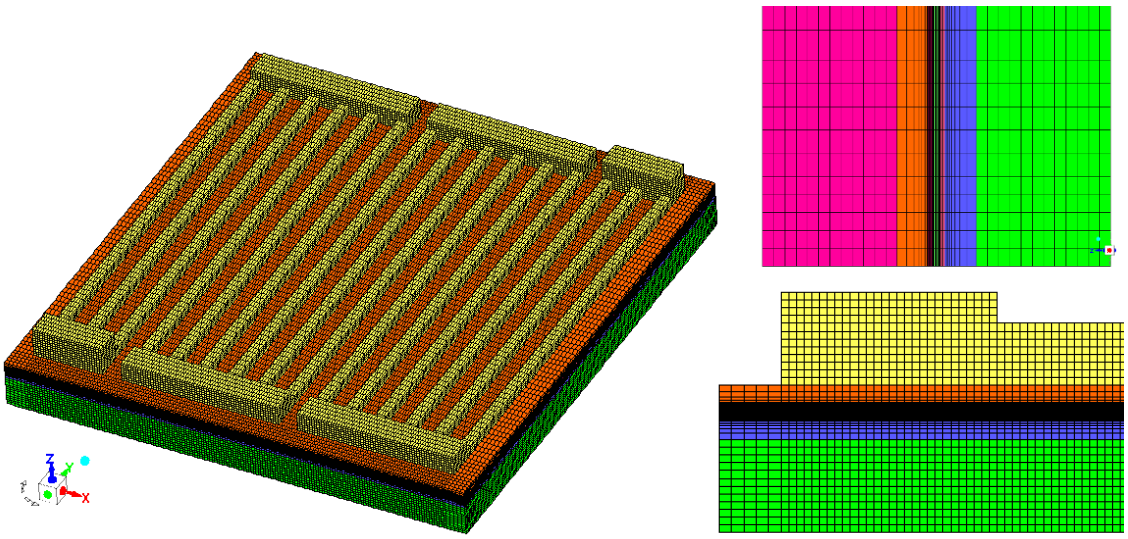

Fig. 2 – Sketch of the PEM fuel cell geometry with the mesh developed.

4. Results and Discussions

A numerical investigation for a 5 cm^2 PEM fuel cell is presented and the performance results with a variable microstructure of the CL (Pt particle diameter, ionomer volume fraction, specific surface area) are reported. It is well known that platinum is by far the most effective element used for PEM fuel cell catalysts, and nearly all current PEM fuel cells use platinum particles on porous carbon supports to catalyze both hydrogen oxidation and oxygen reduction reactions. The main goal in studying the PEMFC catalysts is to maximize the surface area and minimize the loading, and one way to achieve this is by optimizing the size and shape of the platinum particles. The present study gives an insight into the catalyst microstructure influence on PEM fuel cell performance.

4.1 *Model Validation*

The validation of the numerical model, including the catalyst microstructure, was achieved by comparing its prediction against previously obtained experimental data using a 5 cm^2 PEM fuel cell from ElectroChem [33]. Two of the four cases analyzed in the experimental investigation are used for model validation, namely: a fuel cell with the same anode catalyst, Pt/C with 0.2 mg/cm^2 Pt loading, and a modified cathode catalyst: (Case 1) one CL with usual Pt/C having 0.2 mg/cm^2 Pt loading and (Case 2) one CL with mixed Pt/iodine-doped graphene obtained by spraying 0.2 mg/cm^2 Pt on the membrane and 0.2 mg/cm^2 iodine doped graphene on GDL. The cathode catalyst layers obtained have different electrochemical active areas (a_{ECSA}) leading to different microstructure properties. The electrochemical active area measurements were performed by cyclic voltammetry and revealed a value for a_{ECSA} for the mixed catalyst (Case 2) between 82 and 90 m^2/g when the temperature is increasing from 60°C to 90 °C, which is 3 times higher than the commercial Pt/C catalyst from the Case 1 (35 - 38 m^2/g at 60 - 90°C). The value for a_{ECSA} set up in the numerical investigation is 37 m^2/g for the Case 1 catalyst and 87 m^2/g for the Case 2 catalyst. Using Eq. (6) and the catalyst properties, we determine the radius of the Pt particles as 3.78 nm for Case 1 and 1.61 nm for Case 2. The porosity of the catalyst layer calculated using Eqs. (7-10) and the base case conditions (Table 1) is 0.5. Based on these properties, we have performed numerical simulations and experimental tests and the electrochemical performances were recorded as polarization curves (experiments) and dots (CFD simulations), see Fig. 3. The CFD results were plotted as dots since a simulation was run for every potential difference value set up between the anode and the cathode. The polarization curves from the experiments were recorded using an in-house test station, which includes an electrochemical workstation, fuel cell (ElectroChem, USA), DS electronic load

(AMETEK Sorensen SLH 60V/120A 600 W), and humidifier (ARBIN DPHS 10, USA). The operating conditions listed in Table 2 have been used in both the numerical and experimental tests. The flow rates of the reactants in the experimental work were adjusted using flow controllers (Alicat Scientific, USA) and bubble-type humidifier were installed to ensure the necessary humidification.

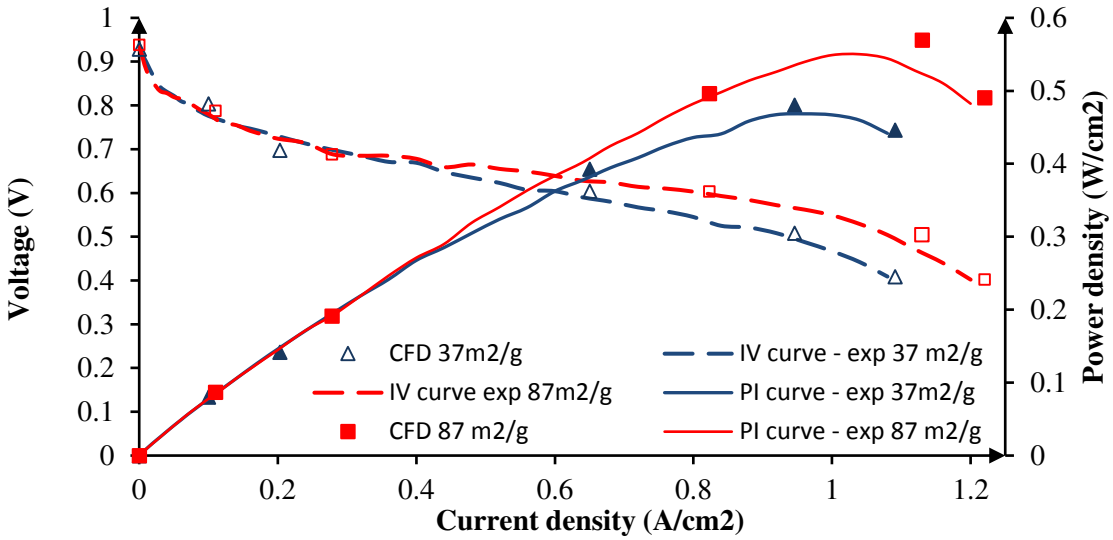

Fig. 3 - Validation of the CFD results with experimental data.

A good agreement between the experimental data and the CFD results have been obtained. It can be noticed that an overall increase in performance of 22 % was achieved by using iodine doped graphene as support for Pt particles and this is due to better electrical contacts and additional pathways for the water removal that have been established. More information about the effect of the carbon support over the PEM fuel cell performance is given in Section 4.2.3. This support based on graphene leads to an increase in the performance in ohmic and concentration polarization regions. At the same time, the higher electrochemical active area, a_{ECSA}, from the Case 2 suggests that more platinum sites are available for the oxygen reduction reaction from the cathode catalyst [33], which leads to a better performance of the fuel cell.

In the second stage of the model validation, we have compared the polarization curves obtained using the model both with and without taking into account the catalyst layer microstructure (CPM-Cathode Particle Model) and the simulations were carried out for a potential difference between 0.938V, the open circuit voltage, and 0.3V, for capturing the mass transfer losses. Thus, we have compared the agglomerate model developed with the simplified homogeneous model, and the results are presented in Fig. 4. As expected, the homogenous model (w/o CPM) overestimates the performance since it does not account for the effect of the mass transport limitation at the agglomerate scale [43], and this result is in agreement with several numerical works [10, 12, 18]. To analyze the differences from the models investigated and how the fuel cell performs locally in each case, we have plotted the oxygen and water mass fractions profiles, and the results are presented in Figs. 5 and 6. It can be noticed that the homogeneous model does not capture the diffusion of the dissolved oxygen nor the water generation, as in the case of the agglomerate model. These gas transport issues are known as concentration losses, both causing the decrease in the PEM fuel cell performance. The generated water captured by the agglomerate model blocks the pores in the catalyst layer so that reactant gases cannot access the active catalyst sites, hence the drop in the cell voltage.

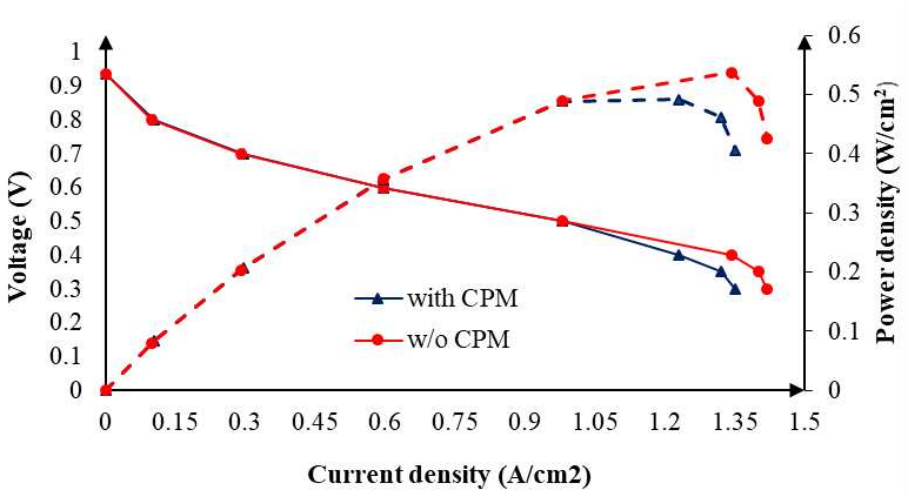

Fig. 4 – Voltage as a function of the current density for the model with and without CL microstructure.

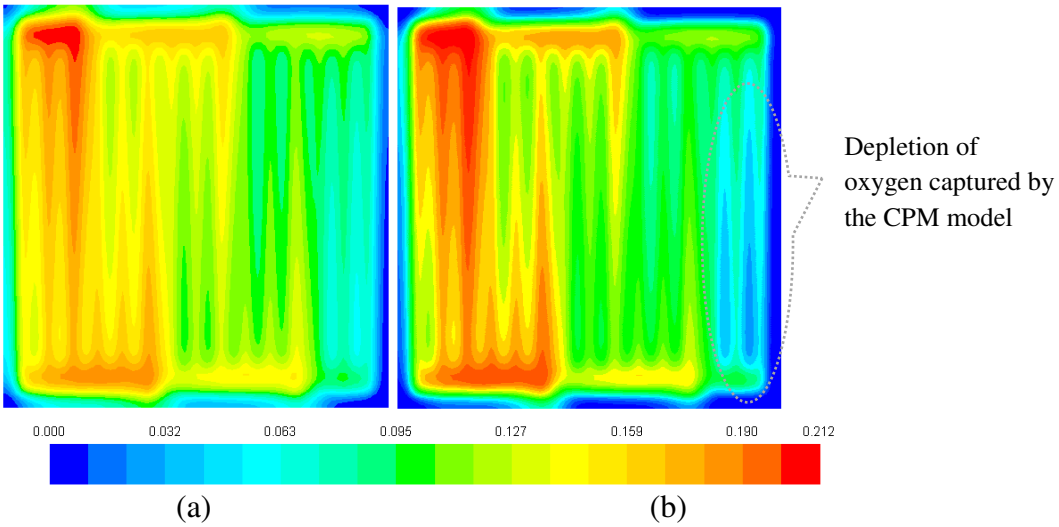

Fig. 5 - Oxygen mass fraction profile for the model (a) without CL microstructure, and (b) with CL microstructure at 0.3V potential difference.

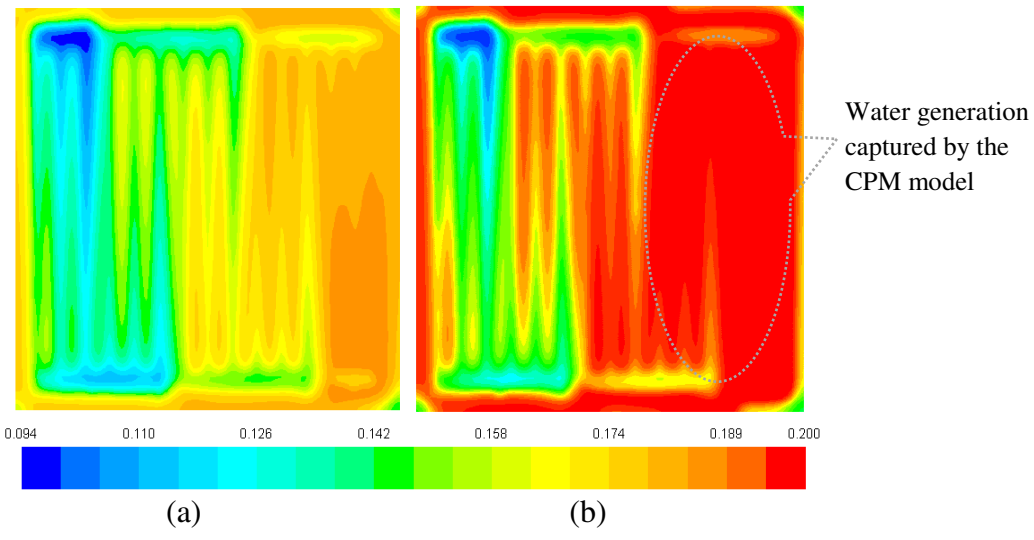

Fig. 6 - Water mass fraction profile for the model (a) without CL microstructure, and (b) with CL microstructure at 0.3V potential difference.

4.2 Effect of the cathode microstructure and composition

In this work we investigate the effect of the following parameters over the PEM fuel cell performance, namely: ionomer volume fractions in the CL ($\varepsilon_{N,CL}$), platinum loading (m_{Pt}), platinum particle radius (r_p) and carbon support. The results were plotted as polarization curves and as profile distributions for the key variables. Since the PEM fuel cell operates at 0.7-0.6 V, the 0.6 V has been chosen as a potential difference for displaying the profiles, unless otherwise specified.

4.2.1 Ionomer volume fraction

The ionomer is added to maintain the hydrophobicity and to bind all the components in the CL and this has an important role in obtaining a good performance of the PEM fuel cell due to its influence on the proton conductivity, gas transport, water management and electron transport. Various ionomer volume fractions have been considered in the study, leading to 6 compositions for the CL. Using the model developed and the base case boundary conditions, the effect of the ionomer volume fraction on the performance was presented in Fig. 6. Increasing the amount of ionomer in the CL, up to 55%, leads to a better performance in the ohmic and concentration regions of the polarization curves. This improvement is due to the fact that the ionomer acts as a network for the mass and charge transport. Increasing the volume fraction of the ionomer above this value leads to a sharp decrease in the catalyst layer porosity ($\varepsilon_{CL} < 0.1$) and hence increase the oxygen mass transport resistance to reach the electrochemical active sites and ultimately leads to the drop in the performance.

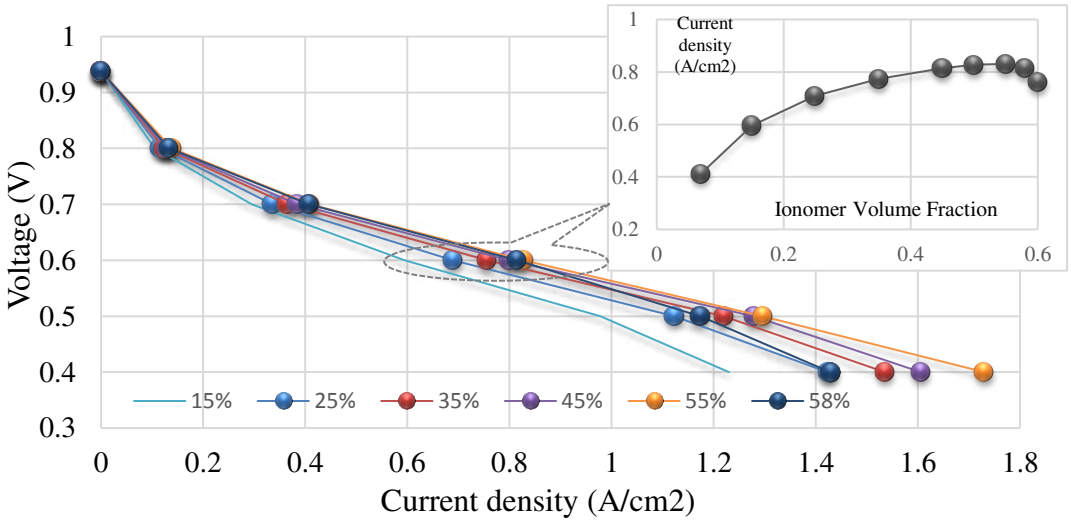

Fig. 7 - Polarization curves for different ionomer volume fractions ($\varepsilon_{N,CL}$).

To establish the optimum value of the ionomer volume fraction, the current density versus ionomer volume fraction have been plotted for all cases investigated at 0.6 V and the results are displayed in the inset plot in Fig. 7. It must be noted that the optimum ionomer volume fraction is the value at which the maximum current density is obtained. It can be observed that there is an optimum range for the ionomer volume fraction, between 45% and 55 %, with the maximum current density 0.83A/cm^2 at 55 %. Sun et al. [44] reported an optimal ionomer volume fraction in CL at ~50%; this result was validated experimentally and is in agreement with the present results. To verify the trend predicted by the model, and due to the fact that there is a decrease in performance (when the ionomer volume fractions is above the optimum value) taking place in the mass transport region of the polarization curve, we have plotted the local distributions of the water content at 0.4V. Water content is the most important variable in investigating the PEM fuel cell performance as almost all property expressions from the CFD model depend on it [38]. As can be seen in Fig. 8, a gradual increase of water content along the channels takes place due to the reactant gas saturation with the water

generated by the cathode electrochemical reaction, for all cases investigated. According to Fuller et al. [45] a completely hydration of the ionomer takes place when the maximum value of the water content is 14, this being the case of a fully saturated vapor phase. In the case of the liquid phase, the maximum value of the water content is 22. If water content is over 14, it is assumed that the flooding phenomenon occurs [46-48]. Excess of ionomer volume fraction (58% case) leads to a maximum water content of 16.2 as compared to the other cases where the maximum are 12.64 (15% case), 13.9 (35% case) and 15.2 (55% case). It can be noticed that for all cases investigated, the maximum value is near the outlet. To verify the flooding phenomena, the liquid water saturation is plotted in Fig. 9. It can be noticed that the largest value of the liquid water saturation appears in the corner close to the exit and that an ionomer volume fraction above the optimum can leads to pore filling with water and consequently to other detrimental effects for the PEM fuel cell performance, such as: blocking the gas diffusion passages, hindering the reactant gases to reach the active sites and decreasing the diffusion rate. These mass transport losses cause the decrease in the fuel cell performance, as presented in the polarization curves from Fig. 7.

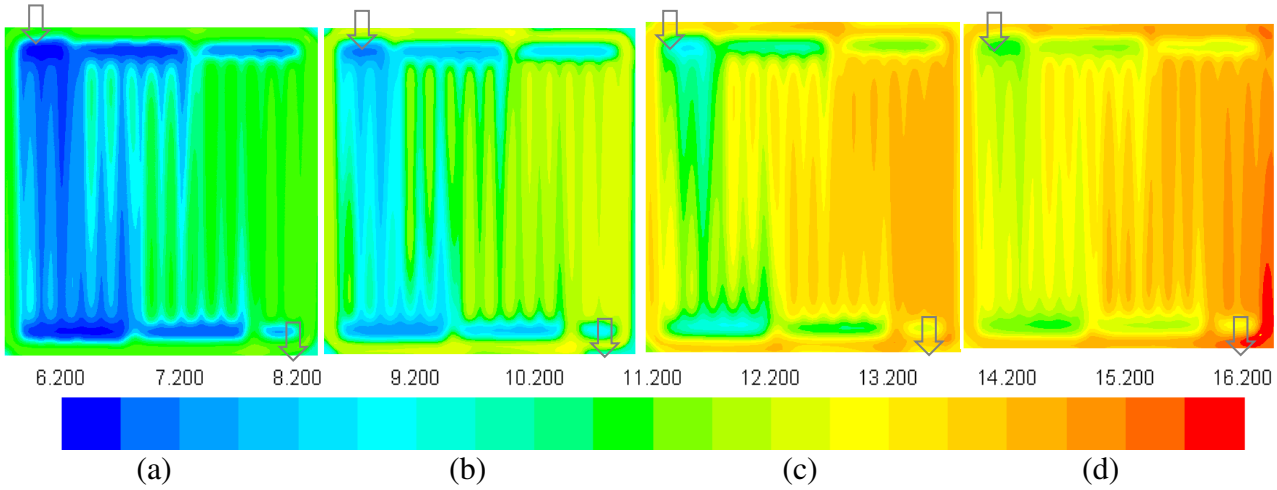

Fig. 8 - Water content profile in the cathode catalyst layer for different ionomer volume fractions at 0.4 V: (a) 15 %, (b) 35 %, (c) 55 % and (d) 58%.

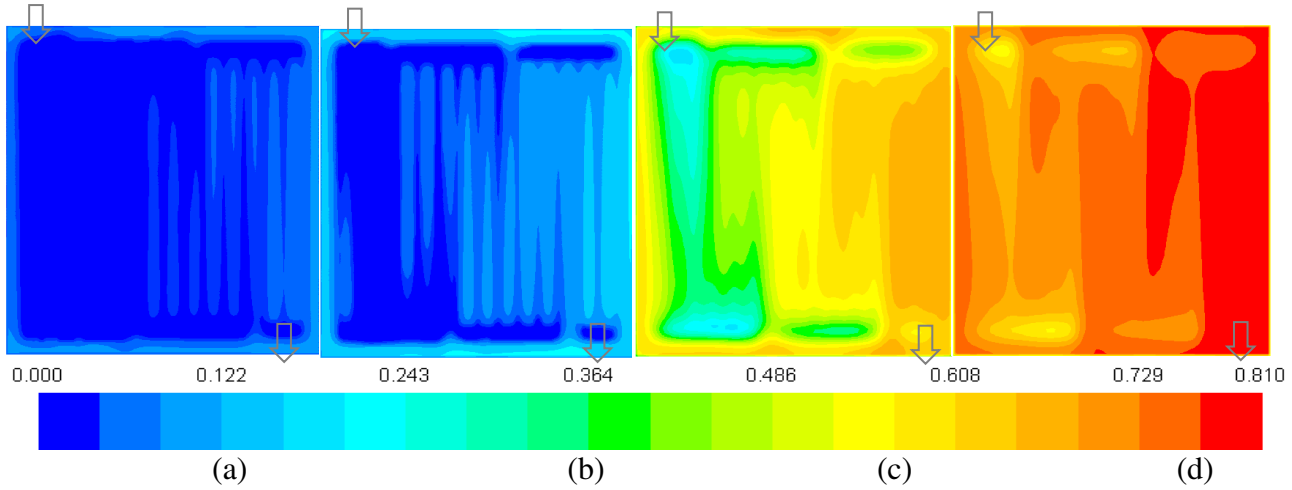

Fig. 9 - Liquid water saturation profile in the cathode catalyst layer for different ionomer volume fractions at 0.4 V: (a) 15 %, (b) 35 %, (c) 50 % and (d) 58%.

4.2.2 Platinum loading and particle radius

The effect of Pt loading and particle radius are taken into account in our investigation because they are the key parameters in improving the electrocatalytic activity and the overall performance of

the PEM fuel cell. Since a platinum supported on carbon catalyst (Pt/C) is formed by a mix of nanometer-sized platinum particles dispersed on a high surface area carbon, ionomer and voids, it is important to establish the influence of each component on the overall performance of the fuel cell. Regarding the platinum loading, the current trend in developing catalyst layers for PEM fuel cells is to reduce it to 0.125 mg_{Pt}/cm^2 or to lower values [23], but at the same time keep the specific active surface area at high values. One way to achieve this goal is by decreasing the size of the platinum particles. In this context, taking into account the model developed, the platinum loading was varied between 0.5 and 4 g_{Pt}/m^2 and the platinum particle radius between 2 and 5.5 nm. Fig. 10 (a) presents the fuel cell performance recorded in terms of current density by taking into account two ionomer volume fractions: the base case (15%) and the optimized case (55 %). It can be noticed that there is an increase in current density for the optimized case of about 28 % as compared to the base case. Further, the profiles for oxygen mass fractions are displayed in Fig. 10 (b)-(e) for the optimized ionomer volume fraction case and using 4 different platinum loadings: 0.05, 1, 2 and 4 g_{Pt}/m^2. The profiles are displayed at the interface between the cathode catalyst layer and the membrane. The oxygen supplied at the cathode channel inlet, see Table 2, and diffuses through the porous layers of the PEM fuel cell to reach the catalyst layer where the electrochemical reactions occur, leading to the oxygen consumption. By using a high platinum loading it can be seen that there is a fast reaction rate for the oxygen reduction reaction and this is due to the additional catalytic surface area provided, as stated by Eq. (5). Hence, a better performance of the fuel cell is obtained, see Fig. 10 (a).

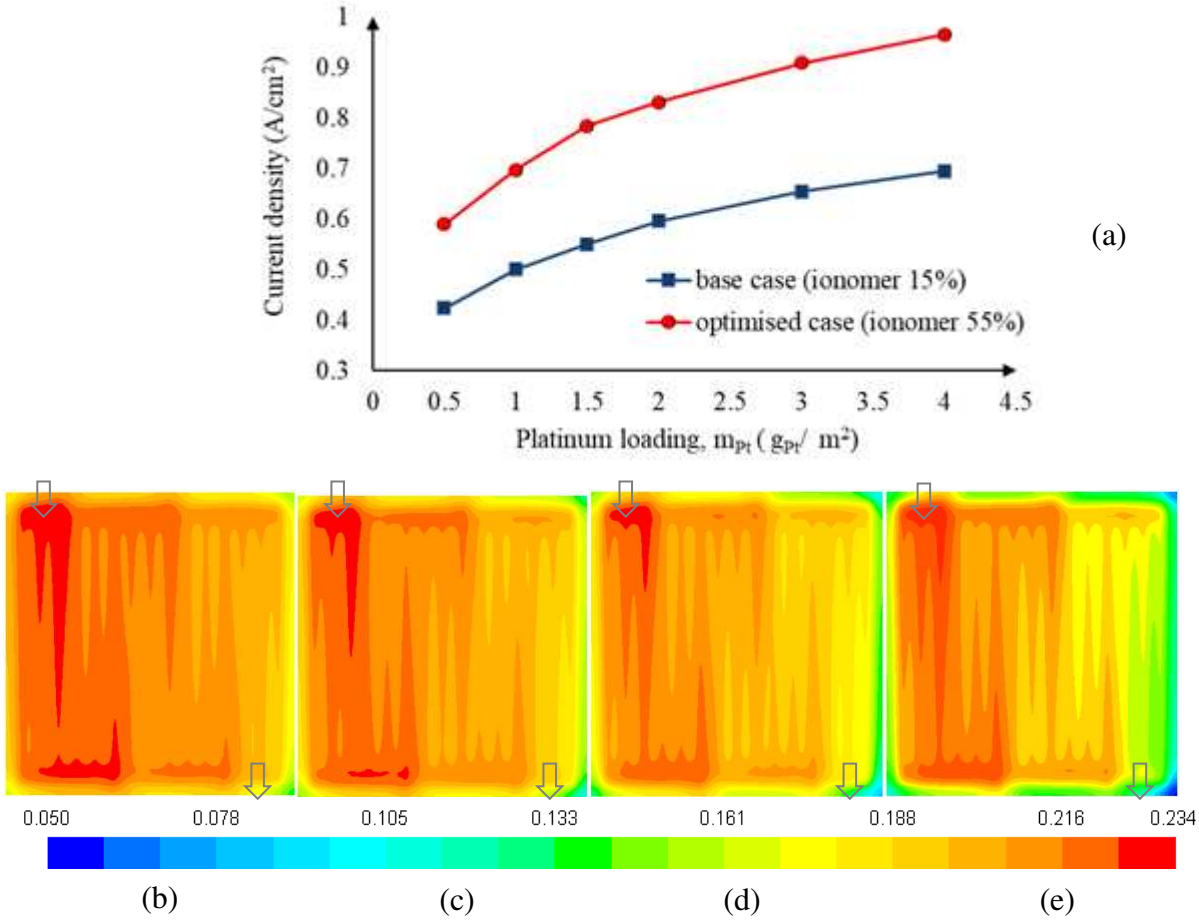

Fig. 10. Platinum mass loading influence on current density (a) and oxygen mass fraction in the CL at 0.6V for optimized ionomer content (55%) for: (b) 0.5 g_{Pt}/m^2, (c) 1 g_{Pt}/m^2, (d) 2 g_{Pt}/m^2 and (e) 4 g_{Pt}/m^2.

Fig. 11 (a) presents the influence of the platinum particles radius over the current density; a decrease in fuel cell performance can be noticed as the radius increases. Essentially, smaller particles

pose smaller resistance to mass transport at the local scale as can be seen in Fig. 11 (b)-(e), where the current density profiles for various particle radius are plotted at the interface between the cathode catalyst layer and the membrane. These results are in agreement with the results from several papers [12, 29] that have reported a range between 2 and 5 nm for obtaining a maximum ORR mass activity and a better performance of the fuel cell. A significant loss in the performance takes place, around 25%, on increasing the radius of the platinum particles from 1.61 nm to 5.5 nm.

The Pt particle size effect on ORR has been widely investigated since 1990 [54] and yet there are several discrepancies in the results, due to different types of electrolytes used in measurements, different electrocatalyst support or experimental conditions [21, 26, 31, 55-57]. A thorough investigation is required to systematically establish the influence of catalyst microstructure and associated parameters on the PEM fuel cell performance. However, decreasing the particle size results in an increased number of sites available on the surface of the catalyst and leads to a larger electrochemical surface area, as shown in Eq. (6). The correlation between the Pt particle size, the catalytic activity and the current density can be seen in Fig. 11 (a) and Fig. 12, where a smaller Pt particle means a higher electrochemical active area and consequently a better performance of the PEM fuel cell. This is in accordance with virtually all the findings of the previous similar studies [17, 24-25, 28].

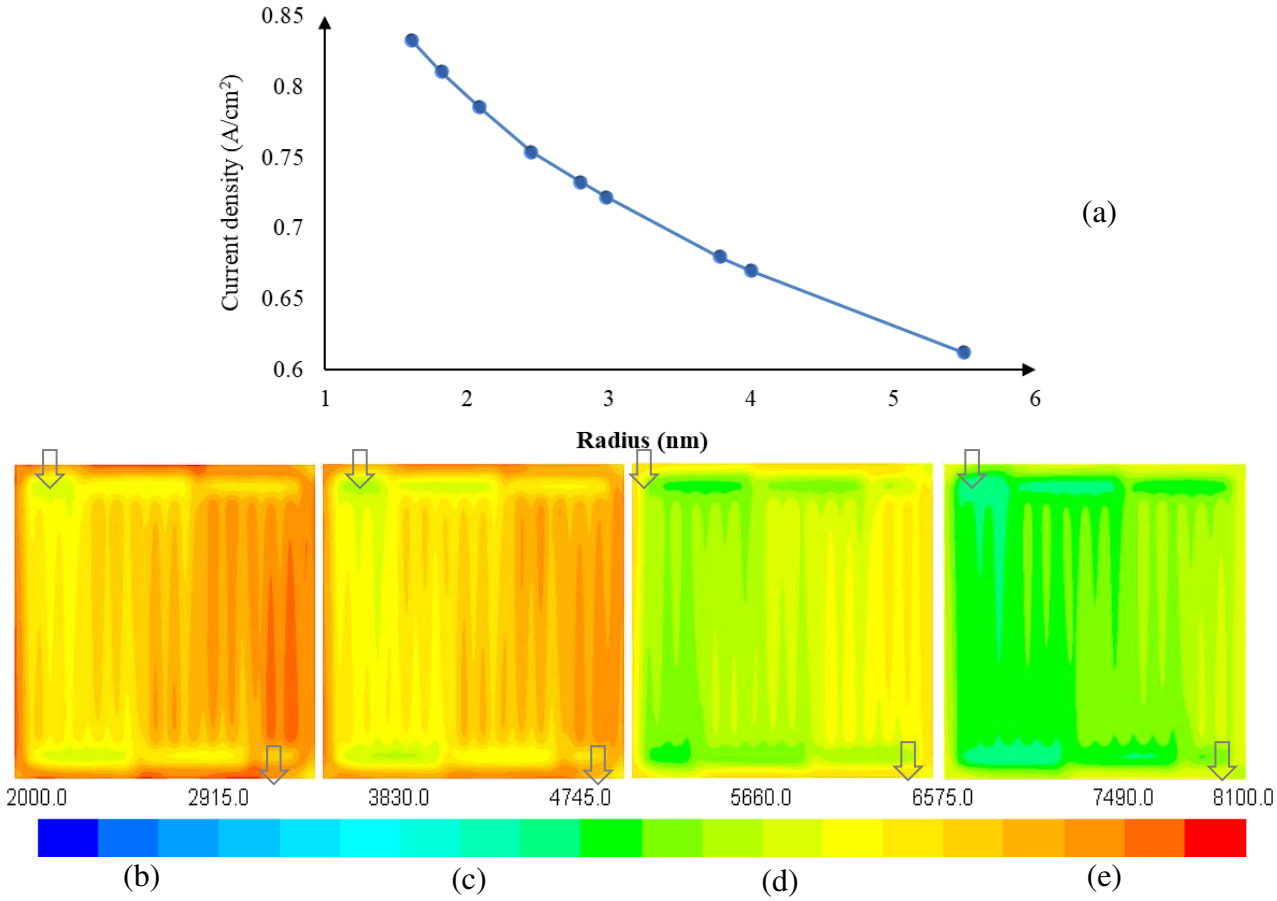

Fig. 11 - The effect of Pt particle radius on (a) average current density and on current density profile for: (b) 1.83nm, (c) 2.45 nm, (d) 3.78 nm and (e) 5.5 nm.

4.2.3 Specific surface area and carbon support

The electrochemical active surface of the catalyst, a_{ECSA}, and the radius of platinum particles, r_p, are correlated according to Eqs. (5-6). The platinum particles are dispersed on the surface of the catalyst support, typically carbon powder (~40 nm) with high meso-porous area (>75m^2/g) [49]. In the last few years, much attention has been paid to finding new catalyst supports and among these carbon materials, graphene has been considered as an excellent support material. Such a

graphene based support has been developed previously by our group [33, 51-53] and investigated experimentally [33]. The numerical and experimental results of PEM fuel cell testing using this catalyst layer and a conventional Pt/C catalyst has been compared in the Section 4.1. The use of iodine-doped graphene as carbon supports in PEM fuel cells has been previously investigated experimentally and numerically [51-53]; the ex-situ and in-situ tests have proven that they are promising materials for PEM fuel cell technology. It must be mentioned that the electrochemical active area, a_{ECSA}, of the above catalysts, was determined by cyclic voltammetry.

To investigate further the effect of the electrochemical active area of the catalyst over the fuel cell performance, we have varied this parameter between 37 m^2/g, obtained for the conventional Pt/C catalyst, and 87 m^2/g, obtained for the mixed catalyst. The results are displayed in Fig. 12, and it is observed that there is an overall 22 % increase in current density as the electrochemical active area is growing. A good agreement between the modelling and experimental data was found, according to results presented in Fig. 3. The substrate effect on the oxygen reduction reaction will be further investigated in order to obtain a better catalyst. Also, the stability and durability of the catalyst will be taken into account in our future work.

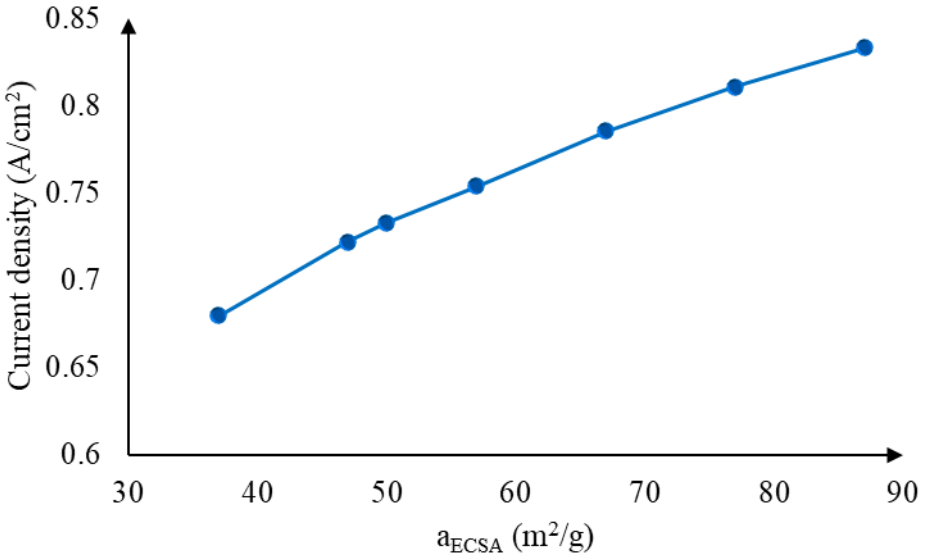

Fig. 12 - Current density (A/cm^2) for various electrochemical active area, a_{ECSA} at 0.6 V.

5. Conclusions

A parametric study has been conducted to primarily investigate the sensitivity of the 5 cm^2 PEM fuel cell performance to the catalyst layer microstructure. A numerical analysis based on ANSYS Fluent 19.0 has been performed and the results have been validated for one parameter against experimental data. The following are the main findings of the study:

1. A comparison between the model results, both with and without taking into account the catalyst microstructure, have been performed. Unlike the agglomerate model, the homogeneous model, which ignores the catalyst microstructure, overestimates the fuel cell performance in the concentration losses region as it does not accurately capture the depletion of oxygen and generation of water.
2. The effect of the cathode microstructure (ionomer volume fraction platinum loading, platinum particle radius, electrochemical active area and carbon support type) is discussed in the paper and the results are plotted as graphs or profiles for investigating their influence over the fuel cell performance. An optimum range for the ionomer volume fraction was found. A higher platinum loading and a lower particle radius are recommended to achieve better PEM fuel cell performance.
3. For one parameter, namely the electrochemical active area a_{ECSA}, the numerical results are validated by experimental data and a good agreement was found. Comparing the results of two catalysts investigated, an overall increase in performance of 22 % was achieved by using

a mixed cathode catalyst, based on iodine doped graphene as support for the Pt particles. This is due to better electrical contacts and additional pathways for water removal.

Acknowledgements

This work was supported by a grant of the Romanian National Authority for Scientific Research and Innovation, CNCS/CCCDI -UEFISCDI, project number PN-III-P2-2.1-PED-2016-1387, within PNCDI III, and by a grant of the Romanian Ministry of Research and Innovation, CCCDI - UEFISCDI, project number PN-III-P1-1.2-PCCDI-2017-0194/25 PCCDI within PNCDI III.

References

[1] Yoon Y-G, Park GG, Yang TH, Han JN, Lee WY, Kim CS. Effect of pore structure of catalyst layer in a PEMFC on its performance. Int J Hydrogen Energy 2003; 28(6): 657-62.

[2] Suzuki A, Sen U, Hattori T, Miura R, Nagumo R, Tsuboi H, Hatakeyama N, Endou A, Takaba H, Williams MC, Miyamoto A. Ionomer content in the catalyst layer of polymer electrolyte membrane fuel cell (PEMFC): Effects on diffusion and performance. Int J Hydrogen Energy 2011; 36(3): 2221-9.

[3] Sohn YJ, Yim SD, Park GG, Kim M, Cha SW, Kim K. PEMFC modeling based on characterization of effective diffusivity in simulated cathode catalyst layer, Int J Hydrogen Energy 2017; 42(10): 13226-33.

[4] Khakaz-Baboli M, Harvey DA, Pharoah JG. Investigating the performance of catalyst layer micro- structures with different platinum loadings. ECS Transactions 2013; 50(2): 765-72.

[5] Obut S, Alper E. Numerical assessment of dependence of polymer electrolyte membrane fuel cell performance on cathode catalyst layer parameters. J Power Sources 2011; 196:1920-31.

[6] Owejan J P, Owejan, J E, Gu W. Impact of Platinum and Catalyst Layer Structure on PEMFC Performance. J Electrochem Soc 2013; 160: F824-33.

[7] Moore M, Wardlaw P, Dobson P, Boisvert JJ, Putz A, Spiteri RJ, Secanell M. Understanding the Effect of Kinetic and Mass Transport Processes in Cathode Agglomerates. J Electrochem Soc 2014; 161:E3125-37.

[8] Weber A Z, Borup RL, Darling RM, Das PK, Dursch TJ, Gu W, Harvey D, Kusoglu A, Litster S, Mench MM, Mukundan R, Owejan JP, Pharoah JG, Secanell M, Zenyuk IV. A Critical Review of Modeling Transport Phenomena in Polymer-Electrolyte Fuel Cells. J Electrochem Soc 2014; 161:F1254-99.

[9] Darling RM. A Hierarchical Model for Oxygen Transport in Agglomerates in the Cathode Catalyst Layer of a Polymer-Electrolyte Fuel Cell. J Electrochem Soc 2018; 165(9):F571-80.

[10] Xing L, Mamlouk M, Kumar R, Scott K. Numerical investigation of the optimal Nafion ionomer content in cathode catalyst layer: An agglomerate two-phase flow modelling. Int J Hydrogen Energy 2014; 39(17): 9087-104.

[11] Soboleva T, Malek K, Xie Z, Navessin T, Holdcroft S. PEMFC catalyst layers: the role of micropores and mesopores on water sorption and fuel cell activity. ACS Appl Mater & Interfaces 2011; 3(6): 1827–37.

[12] Malek K, Mashio T, Eikerling M. Microstructure of catalyst layers in PEM fuel cells redefined:a computational approach. Electrocatalysis 2011, 2(2): 141–57.

[13] Zamel N. The catalyst layer and its dimensionality—a look into its ingredients and how to characterize their effects. J Power Sources 2016; 309: 141–59.

[14] Berning T, Djilali N. A 3D, multiphase, multicomponent model of the cathode and anode of a PEM fuel cell. J Electrochem Soc 2003; 150: A1589 -98.

[15] Wang CY. Fundamental models for fuel cell engineering. Chem Rev 2004; 104: 4727-66.

[16] Sivertsen BR, Djilali N. CFD - based modelling of proton exchange membrane fuel cells. J Power Sources 2005; 141: 65-78.

[17] You L, Liu H. A parametric study of the cathode catalyst layer of PEM fuel cells using a pseudo-homogeneous model. Int J Hydrogen Energy 2001; 26(9): 991-999.
[18] Epting WK, Litster S. A three-dimensional agglomerate model for the cathode catalyst layer of PEM fuel cells. Int J Hydrogen Energy 2012; 37: 8505-11.
[19] Prodip KD, Xianguo L, Zhong-Sheng L, A three-dimensional agglomerate model for the cathode catalyst layer of PEM fuel cells. J Power Sources 2008; 179(1): 186-99.
[20] Marquis J, Coppens MO. Achieving ultra-high platinum utilization via optimization of PEM fuel cell cathode catalyst layer microstructure. Chem Eng Sci 2013; 102:151–62.
[21] Zhang J, Wang Y, Zhang J, Liang J, Lu J, Xu L. The effect of Pt/C agglomerates in electrode on PEMFC performance using 3D micro-structure lattice models. Int J Hydrogen Energy 2017; 42(17): 12559-66.
[22] Harvey D, Pharoah JG, Karan K. A comparison of different approaches to modelling the PEMFC catalyst layer. J Power Sources 2008; 179: 209–19.
[23] DOE Technical Targets for Polymer Electrolyte Membrane Fuel Cell Components, https://www.energy.gov/eere/fuelcells/doe-technical-targets-polymer-electrolyte-membrane-fuel-cell-components
[24] Debe M K. Electrocatalyst approaches and challenges for automotive fuel cells. Nature 2012; 486(7401): 43–51.
[25] Kim H, Kim P, Joo JB, Kim W, Yi J. Fabrication of a mesoporous Pt-carbon catalyst by the direct templating of mesoporous Pt-alumina for the methanol electro-oxidation. J Power Sources 2004; 157(1): 196-200.
[26] Peuckert M, Yoneda T, Betta RAD, Boudart, M. Oxygen Reduction on Small Supported Platinum Particles. J Electrochem Soc 1986; 133(5): 944- 7
[27] Shah AA, Kim GS, Gervais W, Young A, Promislow K, Li J, Ye S. The effects of water and microstructure on the performance of polymer electrolyte fuel cells. J. Power Sources 2006; 160(2) 1251-68.
[28] Khajeh-Hosseini-Dalasm N, Kermani MJ, Ghadiri Moghaddam D, Stockie JM. A parametric study of cathode catalyst layer structural parameters on the performance of a PEM fuel cell. Int J Hydrogen Energy 2010; 35(6): 2417-27.
[29] Kamarajugadda S, Mazumder S. Numerical investigation of the effect of cathode catalyst layer structure and composition on polymer electrolyte membrane fuel cell performance. J Power Sources 2008; 183(2): 629–42.
[30] Afsahi F, Mathieu-Potvin F, Kaliaguine S, Impact of Ionomer Content on Proton Exchange Membrane Fuel Cell Performance. Fuel Cells 2016; 16(1):107-25.
[31] Passalacqua E, Lufrano F, Squadrito G, Patti A, Giorgi L. Nafion content in the catalyst layer of polymer electrolyte fuel cells: effects on structure and performance. Electrochimica Acta 2001; 46(6):799-805.
[32] Antolini E. Carbon supports for low-temperature fuel cell catalysts. Appl Catalysis B: Environmental 2009; 88: 1–24.
[33] Marinoiu A, Raceanu M, Carcadea E, Varlam M, Stefanescu I. Iodinated carbon materials for oxygen reduction reaction in proton exchange membrane fuel cell. Scalable synthesis and electrochemical performances. Arabian J of Chem 2016; https://doi.org/10.1016/j.arabjc.2016.12.002
[34] Hoe LP, Boaventura M, Lagarteira T, Shyuan LK, Mendes A. Polyol synthesis of reduced graphene oxide supported platinum electrocatalysts for fuel cells: Effect of Pt precursor, support oxidation level and pH. Int J Hydrogen Energy (2018); https://doi.org/10.1016/j.ijhydene.2018.05.147
[35] Das E, Gursel SA, Sanli LI, Bayrakceken Yurtcan A. Comparison of two different catalyst preparation methods for graphene nanoplatelets supported platinum catalysts. Int J Hydrogen Energy 2016; 41(23): 9755-61.
[36] Banham D, Feng F, Furstenhaupt T, Pei K, Ye S, Birss V. Novel Mesoporous Carbon Supports for PEMFC Catalysts. Catalysts 2015; 5(3): 1046-67.

[37] Um S, Wang CY, Chen KS. Computational Fluid Dynamics Modeling of Proton Exchange Membrane Fuel Cells. J Electrochem Soc 2000; 147(12) 4485-93.
[38] Carcadea E, Varlam M, Ingham DB, Ismail MI, Patularu L, Marinoiu A, Schitea D. The effects of cathode flow channel size and operating conditions on PEM fuel performance: A CFD modelling study and experimental demonstration. Int J Energy Res 2018;1–16.
[39] Ismail MS, Ingham DB, Ma L, Hughes KJ, Pourkashanian M. Effects of catalyst agglomerate shape in polymer electrolyte fuel cells investigated by a multi-scale modelling framework. Energy 2017; 122: 420-30.
[40] Scholz H. "Modellierung und Untersuchung des Wärme- und Stofftransports und von Flutungsphänomenen in Niedertemperatur-PEM-Brennstoffzellen". PhD Thesis. 2015.
[41] Hao L, Moriyama K, Gu W, Wang C Y. Modelling and experimental validation of Pt loading and electrode composition effects in PEM fuel cells. J Electrochem Soc 2015; 162(8): F854–67.
[42] ANSYS. Multiphysics help, www.ansys.com
[43] Huang J, Li Z, Zhang J. Review of characterization and modeling of polymer electrolyte fuel cell catalyst layer: The blessing and curse of ionomer. J Front Energy 2017; 11(3): 334-64.
[44] Sun YP, Xing L, Scott K. Analysis of the kinetics of methanol oxidation in a porous Pt-Ru anode. J Power Sources 2010; 195(1):1–10.
[45] Fuller TF, Newman J. Experimental Determination of the Transport Number of Water in Nafion 117 Membrane. J Electrochem Soc 1992; 139(5): 1332-7.
[46] Nguyen VD, Lee JK, Kim KC, Ahn JW, Park SH, Kim TU, Kim HM. Dynamic simulations of under-rib convection-driven flow-field configurations and comparison with experiment in polymer electrolyte membrane fuel cells. J Power Sources 2015; 293, 447–457.
[47] Choi KS, Kim HM, Moon SM. An experimental study on the enhancement of the water balance, electrochemical reaction and power density of the polymer electrolyte fuel cell by under-rib convection. Electrochem Commun 2011; 13(12): 1387–90.
[48] Lee B, Park K, Kim HM. Numerical Optimization of Flow Field Pattern by Mass Transfer and Electrochemical Reaction Characteristics in Proton Exchange Membrane Fuel Cells. Int J Electrochem Sci 2013; 8: 219 – 34.
[49] Barbir F. PEM Fuel Cell: Theory and Practice. 2nd ed. Amsterdam; Boston: Elsevier Academic Press; 2012.
[50] Watanabe M, Saegusa S, Stonehart P. Electro-catalytic activity on supported platinum crystallites for Oxygen Reduction in Sulphuric Acid. Chemistry Letters 1988; 17(9): 1487- 90.
[51] Marinoiu A, Raceanu M, Carcadea E, Varlam M , Stefanescu I. Low cost iodine intercalated graphene for fuel cells electrodes, Appl Surf Sci, 2017; 424: 93-100.
[52] Marinoiu A, Gatto I, Raceanu M, Varlam M , Moise C, Pantazi A, Jianu C, Stefanescu I. Low cost iodine doped graphene for fuel cell electrodes. Int J Hydrogen Energy 2017; 42(43): 26877-88.
[53] Marinoiu A, Teodorescu C, Carcadea E, Raceanu M, Varlam M, Cobzaru C, Stefanescu I. Graphene-based materials used as the catalyst support for PEMFC applications. Materials Today: Proceedings 2015; 2: 3797–805.
[54] Kinoshita K. Particle Size Effects for Oxygen Reduction on Highly Dispersed Platinum in Acid Electrolytes. J. Electrochem. Soc. 1990; 137:845–8.
[55] Xu Z, Zhang H, Zhong H, Lu Q, Wang Y, Su D. Effect of particle size on the activity and durability of the Pt/C electrocatalyst for proton exchange membrane fuel cells. Appl. Catal. B Environ. 2012;111–112:264–270.
[56] Shao M., Peles A., Shoemaker K. Electrocatalysis on platinum nanoparticles: Particle size effect on oxygen reduction reaction activity. Nano Lett. 2011;11:3714–3719.
[57] Watanabe M, Saegusa S, Stonehart P. Electro-catalytic Activity on Supported Platinum Crystallites for Oxygen Reduction in Sulphuric Acid. Chem. Lett. 1988; 148:1487-90.